A long non-coding RNA, *afu-254*, is required for the oxidative stress response, cell wall stress response, azole susceptibility and virulence in *Aspergillus fumigatus*

Ritu Devkota[1,2,*], Nava Poudyal[1,2], Jazmin Reyes Servin[3], Julianna Lenz[3], Kelly M. Shepardson[3], and Sourabh Dhingra[1,2,4]

1. Department of Biological Sciences, Clemson University, Clemson, SC, 29634
2. Eukaryotic Pathogen Innovation Center, Clemson University, Clemson, SC, 29634
3. Molecular Cell Biology Department, University of California Merced, Merced, CA, 95343
4. Address correspondence to: sdhingr@clemson.edu

[*] Current affiliation – Research Associate, SystImmune, ritu.devkota15@gmail.com

Abstract:

Long non-coding RNAs play an important role in stress response in all forms of life; however, a tight regulation of lncRNAs is required for normal function. Abnormal expression of lncRNA is associated with uncontrolled cell growth in many forms of cancer. Recent studies have highlighted the role of lncRNAs in *Aspergillus fumigatus* in azole stress response and virulence. Here, using a transcriptome dataset of *A. fumigatus* response to stress, we identified *afu-254* as an 854bp lncRNA that plays a role in modulating oxidative stress, fungal sub-MIC azole response to posaconazole and itraconazole, cell wall stress, macrophage phagocytosis and killing *ex vivo*, and virulence in an invertebrate model of *Aspergillus* infection. Importantly, *afu-254* does not produce cross-azole susceptible response and plays a role in fungal azole response against posaconazole and itraconazole but not voriconazole. Furthermore, we showed that stochiometric levels of *afu-254* are important for its function, and ectopic overexpression of *afu-254* in the WT strain leads to an antimorph. This phenotype may stem from a higher ordered structure that is denatured with heat, indicating the presence of a non-functional isoform. In conclusion, we characterized a novel lncRNA, *afu-254*, that is important for stress response and virulence in the pathogenic fungus *A. fumigatus*.

32 **Importance:**

33 Failure of azole treatment for invasive *Aspergillus* infection by both drug-resistant and drug-
34 sensitive isolates is an area of concern and global importance. Fungal stress response is
35 multifaceted, and long non-coding RNAs have emerged as important players in mediating
36 it, including regulating responses to azole antifungals. Here, we have identified a long non-
37 coding RNA, *afu-254*, that plays a role in modulating fungal response to oxidative stress,
38 cell wall stress, azole stress, immune cell stress and virulence in an invertebrate model of
39 invasive *Aspergillus* infection.

40

41 **Introduction:**

42 *Aspergillus fumigatus*, in the genus *Aspergillus*, is the leading cause of invasive pulmonary
43 aspergillosis (IPA) (1). It is ubiquitous in nature and mainly affects people with a
44 compromised immune system. Factors such as prolonged neutropenia, hematologic
45 malignancy, and prolonged use of corticosteroids have all been linked to the disease;
46 however, patient populations with mild or no immunosuppression are increasingly
47 becoming susceptible (2, 3). The azole class of drugs is the primary choice and frontline
48 treatment for management of IPA that includes voriconazole, posaconazole, itraconazole
49 and isavuconazole (4). However, the recent rise in azole resistance raised the global alarm,
50 resulting in the WHO identifying drug-resistant *A. fumigatus* as a pathogen of critical
51 concern (5). Azole drugs work by interacting with and blocking the Cyp51 enzyme, a Sterol
52 14α-demethylase enzyme, that is part of ergosterol biosynthesis, the primary sterol in *A.*
53 *fumigatus* membrane (6). However, binding affinities of azoles to Cyp51 differ on the basis
54 of their side-chains (7), and mutations in the Cyp51 protein sequence, along with
55 duplication in the promoter region, are the primary resistance mechanisms (8). Different
56 mutations within Cyp51 have been found to affect how drug binding occurs. For example,
57 the G54 mutation in Cyp51 confers resistance to itraconazole and posaconazole but not to
58 voriconazole (9, 10). Structural studies have identified differential binding of the short-tail
59 (voriconazole) vs. long-tail (posaconazole and itraconazole) azole drugs to mutated Cyp51
60 as the reason for the lack of cross-resistance (11). Further, MIC changes for posaconazole
61 and itraconazole correlate owing to their structure (12, 13). Drug binding to the target
62 enzyme is and has been defined as a major contributing factor to drug resistance. However,

63 recently, non-genetic changes including persistence, tolerance and hetero-resistance are
64 also associated with fungal response to azole drugs (14, 15).

65 Long non-coding RNAs (lncRNAs) are becoming increasingly important in regulating
66 non-genetic stress response mechanisms, including drug responses (16). In *A. fumigatus*,
67 we previously showed that an lncRNA, *afu-182*, plays a role in fungal response to azole
68 drugs without a change in its minimum inhibitory concentration (15), where others have
69 also shown a role of ncRNA in drug resistance (17). Additionally, in other fungi like *Mucor*
70 *circinelloides*, RNA mechanisms play a role in drug resistance (18). In *S. pombe*, lncRNA
71 plays a role in response to DNA damaging agents (19).

72 Thus, to test the roles of lncRNAs in stress response, including oxidative stress
73 response, we analyzed the publicly available datasets of lncRNAs in *A. fumigatus* (20–22)
74 and identified that lncRNA *afu-254* was downregulated under oxidative and iron stress
75 individually, and ~90% downregulated in the presence of both stresses (21). Thus, we
76 hypothesized that *afu-254* is important for fungal response to oxidative stress, iron stress
77 and azole response.

78 Here, using rapid amplification of cDNA ends (RACE), we show that *afu-254* is an
79 854bp RNA with a 60 bp intron that plays a role in oxidative stress response and
80 differentially regulates azole response to long-tail azoles. In addition, *afu-254* is required
81 for virulence in an invertebrate model of invasive aspergillosis. Thus, here we characterize
82 an lncRNA that regulates fungal azole response and does not provide cross-resistance to
83 azoles. Future research will determine the *afu-254* interactome mediating these
84 phenotypes.

85 **Results:**

86 ***afu-254* is an 854bp-long non-coding RNA:**

87 To determine the roles of lncRNA in *A. fumigatus* stress response, we identified *afu-254* to
88 be differentially regulated when exposed to oxidative and low iron stress (21). However, *afu-*
89 *254* is currently annotated as 145bp ncRNA (Af293 FungiDB accession no. Afu7g04115)
90 (22). To determine the role of *afu-254*, we first identified the boundaries of *afu-254*. We
91 performed 5' Rapid Amplification of cDNA ends (RACE) and 3' RACE (23). We demonstrated
92 that *afu-254* is a 854 bp lncRNA (sequence-region scf_000008_A_fumigatus_A1163
93 920,444 – 921 357, crick strand) with a 60bp intron (sequence-region
94 scf_000008_A_fumigatus_A1163 920,713– 920,772; crick strand) with a Fickett score of
95 0.39969, a putative ORF of 32 amino acid with zero similarity in Swiss-Prot database , a pI
96 of 9.84 and a coding probability of 0.0149372 (24, 25), thus classifying it as a lncRNA
97 (Figure 1 and Figure S1). The presence of an intron was confirmed with end-point PCR
98 (Figure S1D).

99 ***afu-254* is differentially regulated by oxidative stress and regulates oxidative stress**
100 **response in *A. fumigatus*:**

101 To confirm the differential expression of *afu-254*, we determined the RNA levels of *afu-254*
102 in GMM and GMM + H_2O_2 (3mM) via quantitative RT-PCR. We observed an 85% reduction
103 ($p<0.001$) in *afu-254* RNA levels in the presence of oxidative stress (Figure 1B). To determine
104 the role of *afu-254*, we generated a deletion strain (Δ*afu-254*) and complemented the strain
105 ectopically. We also over-expressed *afu-254* using the *gpdA* promoter from *A. nidulans* as

106 previously described (15). To confirm these strains were correct, we used qPCR to
107 determine the RNA levels of *afu-254* in each strain. We show that there is 4-fold over-
108 expression in the OE-254 strain and no RNA was detected in the Δ*afu-254* strain (Figure S2).
109 We also performed a northern blot to confirm the presence of RNA in the complement
110 strain (Figure S2). To determine the role of *afu-254* in regulating fungal response to oxidative
111 stress, we inoculated strains in top agar as previously described (26), punched a hole in the
112 center upon solidification, and added either 5mM H_2O_2 or 2mM menadione. We incubated
113 the plates for 36 hours and measured the zone of inhibition. Both Δ*afu-254* ($p<0.01$) and
114 OE-254 ($p<0.01$) showed increased zone of inhibition compared to WT, indicating *afu-254* is
115 necessary for *A. fumigatus* to ameliorate oxidative stress (Figures 1C and 1D). The
116 complement strain reverted growth back to WT. Importantly, the OE-254 strain, like Δ*afu-*
117 *254* strain, showed increased susceptibility to oxidative stress. Using a spot assay, by
118 plating *A. fumigatus* conidia in the presence of 3mM H_2O_2, we obtained similar results,
119 further confirming the phenotype (Figure S2). Thus, *afu-254* plays an important role in
120 regulating fungal oxidative stress response.

121 **Overexpression of *afu-254* forms a higher order structure leading to an antimorph:**
122 Δ*afu-254* strain shows significant growth inhibition in the presence of oxidative stress
123 compared to WT (Figure 1C and 1D). Interestingly, the OE-254 strains also showed severe
124 growth attenuation. To confirm the presence of *afu-254* in the OE-254 strain and to
125 determine if the stochiometric levels of *afu-254* are important for its functions, we did a
126 northern blot to determine the quantity and quality of *afu-254* transcript. We demonstrate
127 over-expression in the OE-254 mutant; however, we consistently observed the presence of

128 a band above the expected band of OE-254 (Figure 2A, red arrow). To confirm that the
129 higher order structure is not just a technical artifact due to the increased amount of target
130 RNA present in the solution, we loaded increasing amounts of WT RNA from 10-40μg
131 (Figure 2A). We did not see the higher-order structure at any level of loaded RNA, indicating
132 the second higher band is not an artifact. To identify if this second band is a higher order
133 structure, we heated the samples at 98°C for 15 min and cooled them immediately before
134 gel loading. As evident in Figure 2B, we saw complete denaturation of the higher molecular
135 band, and an increase in the weight of the expected monomeric RNA molecule, indicating a
136 possible higher ordered state with *afu-254* acting as an antimorph when over-expressed,
137 resulting in the same oxidative stress phenotype as the deletion mutant.

138 ***afu-254* regulates posaconazole and itraconazole response but is dispensable for**
139 **voriconazole response:**

140 We have previously shown that *A. fumigatus* lncRNA regulates fungal response to azole
141 drugs (15). Others have shown that oxidative stress response plays a role in azole response
142 (27, 28). Thus, we inoculated WT, Δ*afu-254*, Comp-254 and OE-254 strains in the presence
143 or absence of posaconazole (0.03μg/ml), itraconazole (0.075 μg/ml), and voriconazole
144 (0.2μg/ml). In the presence of posaconazole, Δ*afu-254* strain is 73% more inhibited
145 compared to WT (Figure 3B and 3C, $p<0.0001$, One-Way ANOVA), and the OE-254 strain
146 failed to grow (Figure 3B and 3C, $p<0.0001$, One-Way ANOVA). Similarly, we saw a 74%
147 reduction in the Δ*afu-254* strain in the presence of itraconazole (Figure 3D and 3E,
148 $p<0.0001$, One-Way ANOVA) and like posaconazole, the OE-254 strain failed to grow in the

149 presence of itraconazole (Figure 3D and 3E, $p<0.0001$, One-Way ANOVA). Importantly, no
150 change in voriconazole susceptibility was observed (Figure S3A). Additionally, the
151 minimum inhibitory concentration of azoles did not change as measured by the broth
152 microdilution method (Figure S3B). To confirm this is not the growth stage specific
153 response, we grew the strains as liquid shaking cultures without or with 0.03μg/ml
154 posaconazole and weighed the 24-hour dry biomass. Both Δ*afu-2*54 and OE-254 strains
155 failed to produce biomass under liquid shaking conditions (Figure S3C), indicating the
156 azole susceptibility is not growth condition specific.

157 ***afu-254* regulates surface attachment and is important for azole response in surface**
158 **attached cultures:** To determine if germination is affecting the azole susceptibility
159 phenotypes of *afu-254*, we grew the strains in 24-well plates and allowed the biofilms to
160 develop for 12 hours. After biofilm formation, planktonic cells were washed with PBS and
161 GMM without or with 0.2μg/ml of posaconazole was added to the wells for 8 hours. The
162 wells are washed and stained with crystal violet to determine the attached biomass. The
163 OE-254 strain showed a 63% decrease in surface attachment after 20 hours in the absence
164 of azoles (Figure 3F, $p<0.0001$). Upon treatment with posaconazole, we normalized the
165 biofilms to untreated controls and observed a 25% reduction in Δ*afu-254* biofilms (Figure
166 3G, $p<0.01$, One-Way ANOVA) and 78% reduction in OE-254 biofilms (Figure 3G, $p<0.0001$,
167 One-Way ANOVA) compared to WT. Thus, *afu-254* plays a role in surface attachment and
168 azole response of surface-attached cultures.

169 ***afu-254* regulates cell wall stress response:** Hydrogen peroxide-mediated oxidative
170 stress pathway leads to changes in the cell wall integrity pathway (29). Thus, to determine if
171 *afu-254* plays a role in fungal response to cell wall stress, we incubated the strains in the
172 absence and presence of Congo red, an anionic azo dye that affects cell wall rigidity (30).
173 Δ*afu-254* showed 54% reduction in growth ratio (Figures 4A and 4B, $p<0.0001$, One-Way
174 ANOVA); whereas OE-254 strain showed 40% reduction in growth ratio (Figures 4A and 4B,
175 $p<0.0001$, One-Way ANOVA) compared to WT strains. We did not see a difference when
176 strains were incubated with the echinocandin drug, Caspofungin, indicating a more
177 regulated cell wall stress response (Figure 4C).

178 **OE *afu-254* regulates macrophage uptake and killing *ex vivo*:** Reactive oxygen species
179 are detrimental to *A. fumigatus* conidia and are a major weapon used by innate immune
180 cells, including macrophages, to kill *A. fumigatus* conidia (31, 32). As *afu-254* plays a role in
181 oxidative stress response, we tested the ability of immortalized bone-marrow derived
182 macrophages (BMDMs) to engulf and/or kill conidia using an *ex vivo* adapted FLARE assay
183 and CFU plating assay, respectively (33). For uptake and killing, we incubated conidia from
184 each strain with BMDMs (MOI 5:1) for 3 or 5 hours, respectively. Interestingly, we observe a
185 decrease in uptake of Δ*afu-254* conidia compared to WT but not OE-254 conidia (Figure 4B,
186 $p<0.05$, Kruskal-Wallis test). We also observe a significant increase in OE-254 conidia
187 killing (Figure 5C, $p<0.0001$, Kruskal-Wallis test). The *ex vivo* killing of Δ*afu-254* trends
188 higher than WT but is not statistically significant (Figure 5C, $p=0.3616$, Kruskal-Wallis test).

189 ***afu-254* regulates fungal virulence in the *Galleria mellonella* model of infection:**

190 The ability to deal with oxidative stress and differences in cell wall stress response has
191 been associated with virulence (34, 35). Thus, we determined the virulence of *A. fumigatus*
192 strains in the *G. mellonella* infection model (36). Worms infected with Δ*afu-254* had a
193 median survival time of 82 hours compared to 45.5 hours for WT (Figure 5D, $p<0.0001$, log
194 rank test). Fifty percent of larvae survived in the Δ*afu-254* group compared to 5% survival in
195 the WT group ($p< 0.001$, Figure 5D). On the other hand, 70% larvae infected with the OE-
196 254 strain survived compared to WT (Figure 5D, median survival time – NA, $p<0.0001$, log-
197 rank test). The experiment was repeated three times with similar results. Thus, *afu-254*
198 plays a role in fungal virulence in *G. mellonella* model of infection.

199

200 **Discussion:**

201 Long non-coding RNAs play an important role in stress response in all forms of life, and
202 recent findings have shown their importance in azole response in *A. fumigatus* (15, 17).
203 However, whether lncRNAs play a role in modulating other stresses is not entirely known.
204 To understand the role of lncRNAs in pathogenesis related stress response, we analyzed a
205 previously published transcriptome dataset in the absence or presence of oxidative stress,
206 low-iron stress, and a combination of both stresses (21). Based on the previous
207 transcriptomics results and our qPCR data, we determined that non-coding RNA *afu-254* is
208 highly expressed RNA and shows an 85% reduction in the presence of oxidative stress
209 mediated by H_2O_2 (Figure 1B). However, *afu-254* was predicted to be a 171bp ncRNA, failing
210 to meet the threshold of 200bp to be classified as lncRNA (20, 22). Previously, the ncRNAs
211 in *A. fumigatus* were determined by a cDNA approach, and more recently, during the
212 course of this study, a genome wide characterization of lncRNAs in *A. fumigatus* was
213 reported (17, 20). Importantly, *afu-254* was not characterized as an lncRNA in either of
214 those studies; however, longer RNA transcripts are predicted at the locus (22). We did a 5'
215 and 3' RACE analysis and characterized *afu-254* as an 854bp long ncRNA, and the DNA
216 sequence coding for this ncRNA contains a 60bp intron in the DNA sequence (Figure 1A
217 and S1). Under the conditions tested, we only found one transcript; however, whether
218 splicing variants exist is currently under investigation. Also, 5' RACE is dependent on the
219 ability of reverse transcriptase to amplify full length cDNA (37); and, it is plausible that
220 there is premature elongation termination. However, complementing *afu-254* fragment
221 ectopically reverts the oxidative stress phenotype, cell wall stress phenotype and virulence

222 back to the WT levels (Figures 3, 4 and 5), indicating functionality. Using species-neutral
223 computational models, the *afu-254* transcript is not predicted to be a protein-coding
224 sequence (24) and thus is classified as an lncRNA.

225 As our identification and confirmation showed *afu-254* to be differentially regulated by
226 oxidative stress, we grew the strains in the presence and absence of H_2O_2 and menadione,
227 which produce peroxide and superoxide, respectively. Both Δ*afu-254* and OE-254 strains
228 showed significant reduction compared to WT (Figures 1C and 1D). Various instances in *A*.
229 *fumigatus* biology have shown the stochiometric levels of proteins to be important for their
230 biological function (38); however, this is the first instance where WT levels of an lncRNA are
231 important for its function in *A*. *fumigatus*. To determine if OE-254 strain has a stable
232 transcript, we did northern blot analysis and observed the intact band at the expected size.
233 In addition to the expected band, we also saw a slow-moving band indicating either an *in-*
234 *vitro* artifact, a multimeric complex or a higher-order structure that is partially denatured
235 (Figure 2A, red arrow). LncRNAs assemble into three dimensional secondary structures like
236 stem-loops and cloverleaf, and structural conservation is important for their functions (39–
237 41). Secondary structures can coalesce to form higher order structures like pseudoknots,
238 triplexes and G-quadraplexes (42, 43). lncRNA can also interact with other RNAs, DNAs
239 and proteins to bind to chromatin to exert its function (44) . To determine if this is in fact a
240 higher ordered structure, we boiled the RNA at 98°C for 15 min, followed by rapid cooling
241 on an ice bath before gel loading. We saw an increase in the expected RNA band and a
242 discernible loss of the slow-moving band, indicating loss of higher ordered structure (Figure
243 2B); however, the possibility that it is a DNA/RNA or RNA/RNA hybrid cannot be excluded.

244 Overexpression of lncRNA has long been associated with cancer development and
245 metastasis (45, 46). lncRNAs can act as sponges and decoys that can sequester other
246 regulatory partners from exerting their functions (47). For example, overexpression of
247 lncRNA Xist serves as a competing endogenous RNA (ceRNA) for miR-34a through
248 sponging, leading to overexpression of the MET oncogene that is involved in various
249 cancers (48). In *A. fumigatus*, overexpression of *afu-254* ectopically acts as an antimorph
250 presumably through the formation of a non-functional multimeric form or tertiary structure
251 (49). It is not clear if this effect is due to *afu-254* driven by a constitutively active *gpdA*
252 promoter or over-expression in general. Further studies will focus on inducible promoters
253 to fine-tune the *afu-254* levels for structural and functional analysis.

254 Oxidative stress plays a role in fungal response to azole drugs (21). Previous studies on
255 lncRNAs have shown their roles in azole response (15, 17). Thus, we grew the strains in the
256 presence of voriconazole (short-tailed azole), posaconazole and itraconazole (long-tailed
257 azoles) (11). Surprisingly, we did not see a growth difference in response to voriconazole
258 (Figure S3A), but both Δ*afu-254* and OE-254 strains were hypersusceptible to both
259 posaconazole and itraconazole (Figure 3). We have previously shown that lncRNA *afu-182*
260 regulates pan-azole response (15); however, unlike *afu-182*, *afu-254*'s response is limited to
261 long-tailed azoles only. Previous studies have shown a strong correlation between
262 posaconazole and itraconazole susceptibility attributed to their structural similarities (12,
263 50). Azole cross-resistance in *A. fumigatus* is determined by specific mutations in the
264 Cyp51 sequence. For example, G54 and P216 mutations in Cyp51 result in resistance to
265 posaconazole and itraconazole but not to voriconazole (10, 51). The G448S mutation

266 provides a high level of resistance to voriconazole, but a low level of resistance to
267 posaconazole and itraconazole (52), and amino acid variations at M220 leads to pan-azole
268 resistance (53). Promoter duplication, along with amino-acid substitutions, is also a major
269 driver of pan-azole resistance (8). If this effect is mediated by a direct role in drug-*Cyp51*
270 interaction or by modulating *cyp51* gene expression is an area of further research.
271 However, we show that both deletion and overexpression of *afu-254* (Δ*afu-254* and OE-254
272 strains) play a role in fungal response to azole drugs. In addition to DNA changes, drug
273 efflux also plays a role in azole-resistance, and voriconazole is a known inducer of MDR
274 (multi drug resistant pumps) (54). However, unlike voriconazole, long-chain azoles, owing
275 to their long side chain associate with the membranes more efficiently (55, 56)and
276 posaconazole is thus a poor substrate for MDR pumps (57) . It is plausible that *afu-254*
277 regulate MDR efflux pumps, thus making fungal cells more susceptible to posaconazole
278 and itraconazole but not voriconazole, leading to different intracellular concentrations.
279 Future research will determine the intracellular azole concentrations to ascertain the
280 differential mechanism of action against various azoles. Importantly, this is the second
281 instance reported from our lab where a lncRNA impacts sub-MIC azole response (15).
282 Previously, we have shown that changes in sub-MIC azole response are a precursor to an
283 increase in MIC and impact azole treatment outcomes in a murine model of IPA (15).

284 We also determined the role of *afu-254* in modulating cell-wall stress response. We plated
285 the strains in the presence of Congo red, an anionic azo dye that binds to chitin and blocks
286 the interaction between chitin and β1,3 glucans, thereby weakening the cell wall (30). We
287 saw both Δ*afu-254* and OE-254 strains showing increased susceptibility to Congo red

288 (Figure 4A), however, no difference was observed in response to Echinocandin drug
289 Caspofungin that targets 1-3-β-D-glucan synthase enzyme, *fksA* (58, 59). It is possible that
290 *afu-254* modulates the levels of cell wall macromolecules or only affects chitin and not
291 β1,3,-glucans. However, the cell wall is the primary interaction site for *A. fumigatus* with
292 immune cells, which function via oxidative and non-oxidative mechanisms for fungal
293 conidia killing. As *afu-254* plays a role in mediating oxidative stress response, we
294 performed an *ex vivo* uptake and killing assay using BMDMs. Our data show decreased
295 uptake but efficient killing of Δ*afu-254* conidia, and increased killing of OE-254 conidia by
296 BMDMs (Figure 5). Even though we do see a similar trend in phenotypes in Δ*afu-254* and
297 OE-254 strains, it is possible that due to the higher order structure of the OE-254 strains,
298 the antimorph effect is beyond the phenotypes detected here, and we are currently parsing
299 out these responses. It is possible that an antimorphic allele in the OE-254 strain affects
300 genomic loci with similar functions, resulting in a hypersusceptible phenotype compared
301 to the null mutant (60). As we only observed cell wall stress phenotype in the presence of
302 chitin-interacting Congo red but not Caspofungin, it is possible that cell wall composition
303 is slightly different in Δ*afu-254* and OE-254 strains. Cell wall beta-glucan becomes exposed
304 in swollen and germinating spores and is recognized by Dectin-1 on resident alveolar
305 macrophages (61). This interaction leads to pro-inflammatory cytokine release (62);
306 whereas chitin recognition is immunomodulatory (63). Chitin can shift the immune
307 response from a Th1 to Th2 and can suppress the activity of IL-1 via increased secretion of
308 IL-1Ra (63, 64). In Δ*afu-254* and OE-254, it is possible that different levels of chitin and β
309 glucans are exposed, leading to differential immune response.

310 RNAs mediated mechanisms play a role in fungal pathogenesis in plants, insects and
311 mammals using varying mechanisms(65–67). Thus, to further understand if the *ex vivo*
312 immune response plays a role in virulence, we used the *Galleria mellonella* model of
313 infection, which has been used as a heterologous host to study host-pathogen interaction
314 (36). Here, we infected the larvae with the WT, Δ*afu-254*, Comp-254 and OE-254 strains of
315 *A. fumigatus*. We observed significantly reduced mortality in larvae infected with Δ*afu-254*
316 and OE-254 strains that correlate with the *ex vivo* data (Figure 5D). It is important to note
317 that catalase-deficient mutants and superoxide dismutase mutants that detoxify peroxides
318 and superoxide, respectively, do not show virulence defects in animal models (68, 69);
319 whereas, oxidation resistance protein 1 (OxrA) leads to virulence attenuation (70). It is well
320 established that *A. fumigatus* has a diverse set of mechanisms to detoxify ROS; however,
321 what genes, if any, are regulated by *afu-254* is not clear. In the future, we plan to study the
322 whole transcriptome response in Δ*afu-254* and OE-254 strains compared to the WT strain.
323 In conclusion, we identified that *afu-254* is a long non-coding RNA that plays a role in
324 fungal response to oxidative stress, cell wall stress and virulence. Additionally, *afu-254*
325 modulates fungal azole response to posaconazole and itraconazole but not voriconazole
326 both in surface and attached cultures. The exact mechanisms of this lack of cross-
327 resistance phenomenon are not clear, and further investigations, both technical and
328 mechanistic, are required to study and understand the roles of lncRNAs in regulating fungal
329 azole response.
330
331

332 **Materials and Methods:**

333 **Rapid amplification of cDNA ends (RACE).** 5' RACE was done using 5' RACE system for
334 rapid amplification of cDNA ends from Invitrogen. Briefly, total RNA was isolated from
335 CEA10 strain as previously described (71). Briefly, *A. fumigatus* strains (10^6 spores/ml) were
336 grown in 50ml of Glucose minimal media (GMM) (72) for 24 h at 37 °C with constant
337 shaking at 250 rpm. For total RNA isolation, mycelia were collected via filtration and rapidly
338 frozen in liquid nitrogen. Frozen samples were pulverized in AGPC (Acid Guanidinium
339 Thiocyanate Phenol Chloroform) solution with 2.3mm silica-zirconia beads in a bead-
340 beater. Samples were centrifuged to remove the insoluble material. Two hundred µl of
341 chloroform was added per ml of AGPC (71) and centrifuged. We collected the aqueous
342 phase and added an equal volume of 70% ethanol, and transferred the mixture to a silica
343 column (Epoch Life Sciences) to bind RNA to the silica membrane via centrifugation at
344 12,000g. Columns were washed with 70% ethanol twice and were completely dried. RNA
345 was eluted in 50µl of nuclease free water. RNA quality was assessed via gel electrophoresis
346 and was quantified with Qantas Fluorometer (Promega, USA) per manufacturer's
347 recommendations.

348 Gene specific primer, SD284, was used for first strand synthesis. cDNA was tailed with
349 dCTP and was amplified with UAP (Invitrogen, Thermo Fisher) and SD366.

350 3' RACE was done as previously described (23). Briefly, first strand cDNA was synthesized
351 using the Superscript II enzyme with primer Qt. *afu-254* was amplified with primers Q_0 and
352 SD78.

353 The resulting fragments were ligated into the pJET1.2 vector (Thermo Fisher) and were
354 sequenced using pJET sequencing primers per the manufacturer's protocol (Thermo Fisher,
355 USA).

356 **Strain generation:** All strains and primers used in this study are listed in Supplementary
357 Table 1 and Supplementary Table 2 respectively. CEA17, a uridine/ uracil auxotrophic
358 derivative of CEA10 was used as the host strain for creating the *Δafu-254 strain* used in this
359 study (73). Briefly, a 1kb region upstream and downstream of the predicted *afu-254*
360 sequence was amplified using primers SD266 and SD267 and SD218 and SD219. A
361 fragment encoding the 5'-orotodine decarboxylase gene from *A. parasiticus* was amplified
362 from pSD38.1 using primers SD1 and SD2. The three resulting fragments were fused via
363 PCR using primers SD222 and SD437.

364 To obtain the complement *afu-254* plasmid*,* DNA fragment corresponding to the *afu-254*
365 transcript was amplified with primers SD580 and SD581 that harbor AscI and Not1
366 restriction sites, respectively. The resulting PCR fragment was digested with AscI and NotI
367 and was ligated into plasmid BS311 harboring the hygromycin resistance gene that was
368 previously digested with AscI and NotI (15).

369 To generate an over-expression strain, *A. nidulans gpdA* promoter just before the TSS was
370 amplified using primers SD134 and SD103 using *A. nidulans* gDNA as the template(74). The
371 DNA sequence corresponding to *afu-254* transcript was amplified using SD 468 and SD202
372 with *A. fumigatus* gDNA as the template. These fragments were fused together via fusion
373 PCR using primers SD136 and SD323 that harbor AscI and NotI sites. The resulting

374 fragment was ligated into plasmid pSD18.1, which contains the *pyrG* gene as a fungal
375 selection marker, previously digested with AscI and NotI.

376 DNA was transformed into the protoplast using polyethylene glycol mediated
377 transformation as previously described (75).

378 **DNA Isolation:** DNA was isolated as described previously. Briefly, *A. fumigatus* spores were
379 inoculated into liquid YGT (0.5% Yeast Extract, 2% Glucose, 1X Hunter's Trace Elements
380 (76)) and incubated overnight as stationary cultures. Fungal mycelium was harvested
381 lyophilized. Dry mycelium was pulverized with 2.3mm silica beads in a bead beater. 1 ml of
382 LETS (0.1 M LiCl, 10 mM EDTA, 10 mM Tris-Cl, pH 8.0 and 0.5% SDS) Buffer. The samples
383 were centrifuged and 600µl of supernatant was mixed with equal volume of
384 phenol:chloroform:iso amyl alcohol (25:24:1). The mixture was centrifuged at 12,000g.
385 Aqueous phase was collected and DNA was pelleted at 4°C with 2.5x volume of 100%
386 Ethanol. DNA pellet was washed with 70% ethanol, dried and resuspended in 50µl of
387 nuclease free water. DNA quality was assessed with gel electrophoresis.

388 **Southern blot:** Southern blot was done using standard techniques (77). Briefly, ten µg of
389 DNA was digested with EcoRV per manufacturer's recommendation (New England
390 Biolabs), run on a 1% agarose gel, and transferred to a positively charged Nylon membrane
391 (Roche, USA) and UV-crosslinked. Membrane was pre-hybridized in EasyHyb, probed with
392 DIG labelled probe and was detected using anti-DIG antibody per manufacturer's
393 recommendations (Roche) . CDP-Star (Roche) was used as a substrate and
394 chemiluminescent image was acquired with Azure C300 imaging system.

395 **Quantitative RT PCR:** RNA was isolated as described above (71). RNA was quantified using
396 a NanoDrop and Quantus fluorometer (Promega). RNA quality was assessed on 1% TAE-
397 agarose gel. Five μg of total RNA treated with RNase-free DNase I (Thermofisher) according
398 to the manufacturer's instructions.

399 For RT-qPCR, 1 μg of RNA was used for first-strand synthesis using MMLV-reverse
400 transcriptase (Promega) per the manufacturer's instructions. Second-strand synthesis and
401 quantitative real-time PCR were performed using iTaq Universal SYBR mix (BioRad) in the
402 CFX Connect Real-Time System (Bio-Rad). *afu-254* transcript levels were quantified using
403 primers SD 324 and SD 325. Histone H4 was used for normalization, and transcript levels
404 were quantified using primers SD 375 and SD 376. Student's t-test was used to compare
405 the difference in the mean.

406 **End-point PCR using cDNA template –** RNA was isolated and treated with DNase as
407 described above. One μg of RNA was converted into cDNA using SuperScript IV reverse
408 transcriptase. Primers SD 201 and SD 78 were used for endpoint PCR. CEA10 gDNA was
409 used as the control.

410 **Northern Analysis:** For northern analysis, RNA was isolated as above. Indicated amounts
411 of RNA was loaded onto 1.2% agarose – 2.2M formaldehyde gel and blotted on positively
412 charged nylon membrane. DIG labelled probe were synthesized with primers SD201 and
413 SD188 using PCR DIG probe synthesis kit per manufacturer's recommendations. The
414 membrane was incubated with the probe overnight at 42°C overnight in DIG EasyHyb
415 (Roche). The probe was washed, and incubated with DIG antibody per manufacturer's

416 recommendation (Roche). The membrane was incubated with ready to use CDP STAR
417 substrate (Roche) and chemiluminescence was visualized using Azure C300
418 chemiluminiscent imaging system.

419 **Stress test:** To test the role of *afu-254* in oxidative stress, cell membrane stress and cell
420 wall stress response in *A. fumigatus*, serial spore dilutions of indicated strains were
421 prepared and inoculated on the plate containing indicated stresses along with no stress
422 control for 48 hours at 37°C, 5% CO_2. Colony diameter was measured, and statistical
423 analysis was performed using GraphPad Prism.
424 Punch hole assay was performed as previously described (38). Briefly, 10^5 spores per ml in
425 5ml of top agar were plated on GMM plates. After solidification, a filter pipette tip (200µL)
426 was used to core out the centre of the plate. 100µl of either 5% H_2O_2 or 2mM Menadione
427 were added and zone on inhibition was measured.
428 All experiments were performed in triplicate and were repeated three times. One-Way
429 ANOVA was used to compare sample means, followed by Tukey's post-hoc analysis.

430 **Broth microdilution assay to determine minimum inhibitory concentration:** Spore
431 suspensions were adjusted to 5 x 10^5 spores per ml and 100µl of spores was added to
432 100µl of drug in GMM in a 96 well plate (16µg/ml – 0.0156µg/ml). The first well showing no
433 fungal growth was recorded as MIC.

434 **Biofilm assay:** In a 24-well plate, 1 ml of GMM containing 10^5 spores of *A. fumigatus* strains
435 was added. The plates were centrifuged at 250 g for 10 minutes and incubated at 37°C for
436 twelve hours. The culture supernatant was removed, and wells were washed twice with

437 PBS and stained with 2 ml of 0.1% crystal violet for 10 min. GMM without or with 0.2μg/ml
438 of posaconazole was added for 8 hours. Wells were then washed twice using autoclaved
439 water to remove excess Crystal violet and treated with 1.5 ml of 100% ethanol for 10
440 minutes. 75 µl of suspension from each well was transferred to the 3 wells of 96 well plate,
441 and absorbance at 600 nm was read using a MultiSkan Sky High Microplate
442 Spectrophotometer. To calculate biofilm formation, the background reading was
443 subtracted from the test reading. For azole treated samples, the absorbance was
444 normalized to untreated controls. One-Way ANOVA was used to compare sample means
445 followed by Tukey's post-hoc analysis.

446 ***Ex vivo* killing Assay:** Immortalized C57BL/6 BMDMs (BEI resources; NR-9546) were used
447 for the macrophage killing assay. Briefly, BMDMs were plated at $0.5x10^6$ cells/well in a 12-
448 well plate. The next day conidia from the indicated strains, at a ratio of 5:1 (conidia:cells),
449 were added to the BMDMs, centrifuged at 1000rpm for 2 minutes, and then incubated for 5
450 hours at 37°C, 5% CO_2. Following incubation, cells were lysed for 2 minutes using ice-cold
451 water. Serial dilutions of the wells were made in PBS and plated on GMM plates. Plates
452 were incubated at 37°C for 48 hours and CFUs were counted.

453 **Macrophage uptake assay:** BMDMs were plated at $0.5x10^6$ cells/well in a 12-well plate.
454 The next day, conidia biotinylation protocol from (33) was used to label each strain with
455 AF633. Briefly, conidia from each of the 4 strains were rotated in Biotin-XX, SSE at a final
456 concentration of 5μg/ml in 50 mM carbonate buffer for 1 hr. Following incubation, unbound
457 biotin was neutralized using 0.1 M Tris- HCL and rotated at room temperature for 15

458 minutes. Conidia were then resuspended in PBS with 0.02 mg/ml of AF633, incubated for
459 45 minutes with constant rotation, and protected from light until experimental use.
460 Following labeling, each of the 5 biotinylated strains were added to the corresponding wells
461 at a ratio of 5:1 (conidia: cell) and incubated for 3 hours at 37°C, 5% CO_2. After incubation,
462 wells were washed with PBS and suspended in Fluorescence activated cell sorting (FACS)
463 buffer (1% Fetal Bovine Serum-PBS). Wells were gently scraped with a cell scraper to
464 resuspend BMDMs. Cells were stained with DAPI for L/D detection and were analyzed using
465 the BD LSR II flow cytometer. Gating on BMDM uptake (AF633+) vs. empty BMDMs (AF633-)
466 was used to quantify total uptake and percentage of BMDM uptake for each strain.

467 Data for CFU and uptake represent combined data from 3 experiments (each with 4-5
468 replicates) and were analyzed with Prism using the Kruskal-Wallis test with Dunn's multiple
469 comparisons.

470 ***Galleria mellonella* infection:** A total of 20 *Galleria mellonella* larvae of cream-white color
471 and similar size were used per strain of *A. fumigatus*. Ten µl containing $5x10^4$ spores was
472 injected directly via Hamilton syringe to the hemocoel as previously described (36). 10 µl of
473 PBS was administered to the control group to ensure PBS was free from contamination.
474 Additionally, 10 worms that were neither infected nor stabbed were used as a control to
475 check for the quality of the worms. After injection, larvae were incubated at 37°C until 5
476 days. For survival analysis, larvae were monitored 3 times daily post-injection. The death of
477 larvae was ensured by a lack of movement upon physical stimuli. Log-rank test was

performed to determine the survival distribution using GraphPad Prism software. The experiment was done three times with similar results.

Statistical Analyses: Non-parametric (Kruskal-Wallis and Log-rank respectively) tests were used for *ex vivo* assay and *G. mellonella* virulence assay. Parametric tests (Student's t-test or One-Way ANOVA followed by Tukey's post-hoc test) were used for other comparisons. GraphPad Prism version 10 was used for all statistical analyses. *$p<0.05$, **$p<0.01$, ***$p<0.001$, ****$p<0.0001$

Acknowledgements:

We would like to acknowledge members of the Dhingra laboratory and the Eukaryotic Pathogen Innovation Center for discussions surrounding the experiments in the manuscript. The research in the Dhingra lab is supported by start-up funds from the Department of Biological Sciences at Clemson University and a National Institute of General Medical Sciences (NIGMS) award (P20GM146584) (PI - James Morris). The funding sources had no role in the study design, data collection and interpretation, preparation of this manuscript or the decision to submit the manuscript. We acknowledge the UC Merced Stem Cell Instrumentation Foundry for assistance in generating flow cytometry data.

496 References:

497 1. Earle K, Valero C, Conn DP, Vere G, Cook PC, Bromley MJ, Bowyer P, Gago S. 2023.
498 Pathogenicity and virulence of *Aspergillus fumigatus*. Virulence 14:2172264.

499 2. Abers MS, Ghebremichael MS, Timmons AK, Warren HS, Poznansky MC, Vyas JM. 2016.
500 A Critical Reappraisal of Prolonged Neutropenia as a Risk Factor for Invasive Pulmonary
501 Aspergillosis. Open Forum Infect Dis 3:ofw036.

502 3. Tio SY, Chen SC-A, Hamilton K, Heath CH, Pradhan A, Morris AJ, Korman TM, Morrissey
503 O, Halliday CL, Kidd S, Spelman T, Brell N, McMullan B, Clark JE, Mitsakos K, Hardiman
504 RP, Williams P, Campbell AJ, Beardsley J, Van Hal S, Yong MK, Worth LJ, Slavin MA.
505 2023. Invasive aspergillosis in adult patients in Australia and New Zealand: 2017-2020.
506 Lancet Reg Health West Pac 40:100888.

507 4. Patterson TF, Thompson GR, Denning DW, Fishman JA, Hadley S, Herbrecht R,
508 Kontoyiannis DP, Marr KA, Morrison VA, Nguyen MH, Segal BH, Steinbach WJ, Stevens
509 DA, Walsh TJ, Wingard JR, Young J-AH, Bennett JE. 2016. Practice Guidelines for the
510 Diagnosis and Management of Aspergillosis: 2016 Update by the Infectious Diseases
511 Society of America. Clin Infect Dis 63:e1–e60.

512 5. WHO fungal priority pathogens list to guide research, development and public health
513 action. https://www.who.int/publications/i/item/9789240060241. Retrieved 19
514 September 2025.

515 6. Lee Y, Robbins N, Cowen LE. 2023. Molecular mechanisms governing antifungal drug
516 resistance. npj Antimicrob Resist 1:5.

517 7. Shi N, Zheng Q, Zhang H. 2020. Molecular Dynamics Investigations of Binding
518 Mechanism for Triazoles Inhibitors to CYP51. Front Mol Biosci 7:586540.

519 8. Dhingra S, Cramer RA. 2017. Regulation of Sterol Biosynthesis in the Human Fungal
520 Pathogen *Aspergillus fumigatus*: Opportunities for Therapeutic Development. Front
521 Microbiol 8:92.

522 9. Diaz-Guerra TM, Mellado E, Cuenca-Estrella M, Rodriguez-Tudela JL. 2003. A Point
523 Mutation in the 14α-Sterol Demethylase Gene cyp51A Contributes to Itraconazole
524 Resistance in *Aspergillus fumigatus*. Antimicrobial Agents and Chemotherapy 47:1120–
525 1124.

526 10. Vazquez JA, Manavathu EK. 2016. Molecular Characterization of a Voriconazole-
527 Resistant, Posaconazole-Susceptible *Aspergillus fumigatus* Isolate in a Lung Transplant
528 Recipient in the United States. Antimicrobial Agents and Chemotherapy 60:1129–1133.

529 11. Sagatova AA, Keniya MV, Tyndall JDA, Monk BC. 2018. Impact of Homologous
530 Resistance Mutations from Pathogenic Yeast on *Saccharomyces cerevisiae* Lanosterol
531 14α-Demethylase. Antimicrobial Agents and Chemotherapy 62:10.1128/aac.02242-17.

532 12. Mosquera J, Denning DW. 2002. Azole Cross-Resistance in *Aspergillus fumigatus*.
533 Antimicrob Agents Chemother 46:556–557.

534 13. Pfaller MA, Messer SA, Boyken L, Rice C, Tendolkar S, Hollis RJ, Diekema DJ. 2008. In
535 Vitro Survey of Triazole Cross-Resistance among More than 700 Clinical Isolates of
536 Aspergillus Species. J Clin Microbiol 46:2568–2572.

537 14. Scott J, Valero C, Mato-López Á, Donaldson IJ, Roldán A, Chown H, Rhijn NV, Lobo-Vega
538 R, Gago S, Furukawa T, Morogovsky A, Ami RB, Bowyer P, Osherov N, Fontaine T,
539 Goldman GH, Mellado E, Bromley M, Amich J. 2023. *Aspergillus fumigatus* Can Display
540 Persistence to the Fungicidal Drug Voriconazole. Microbiology Spectrum
541 https://doi.org/10.1128/spectrum.04770-22.

542 15. Poudyal NR, Mehlem RT, Doneparthi P, Cady T, Willger SD, Ortiz M, Noorai RE, Stajich
543 JE, Dhingra S. 2025. A long non-coding RNA regulates triazole antifungal susceptibility
544 and virulence in *Aspergillus fumigatus*. bioRxiv
545 https://doi.org/10.1101/2025.10.16.682787.

546 16. Mattick JS, Amaral PP, Carninci P, Carpenter S, Chang HY, Chen L-L, Chen R, Dean C,
547 Dinger ME, Fitzgerald KA, Gingeras TR, Guttman M, Hirose T, Huarte M, Johnson R,
548 Kanduri C, Kapranov P, Lawrence JB, Lee JT, Mendell JT, Mercer TR, Moore KJ, Nakagawa
549 S, Rinn JL, Spector DL, Ulitsky I, Wan Y, Wilusz JE, Wu M. 2023. Long non-coding RNAs:
550 definitions, functions, challenges and recommendations. Nat Rev Mol Cell Biol 24:430–
551 447.

552 17. Bowyer P, Weaver D, Qi T, Chown H, Fraczek M, Lebedinec R, Dineen L, Valero C, Rhijn
553 N van, Furukawa T, Bromley M, Delneri D. 2025. Genome-wide discovery and

554 phenotyping of non-coding transcripts in *A. fumigatus* reveals lncRNAs with a role in
555 antifungal drug sensitivity https://doi.org/10.21203/rs.3.rs-6048166/v1.

556 18. Chang Z, Billmyre RB, Lee SC, Heitman J. 2019. Broad antifungal resistance mediated
557 by RNAi-dependent epimutation in the basal human fungal pathogen Mucor
558 circinelloides. PLoS Genet 15:e1007957.

559 19. Ard R, Tong P, Allshire RC. 2014. Long non-coding RNA-mediated transcriptional
560 interference of a permease gene confers drug tolerance in fission yeast. 1. Nat
561 Commun 5:5576.

562 20. Jöchl C, Rederstorff M, Hertel J, Stadler PF, Hofacker IL, Schrettl M, Haas H,
563 Hüttenhofer A. 2008. Small ncRNA transcriptome analysis from *Aspergillus fumigatus*
564 suggests a novel mechanism for regulation of protein synthesis. Nucleic Acids
565 Research 36:2677–2689.

566 21. Kurucz V, Krüger T, Antal K, Dietl A-M, Haas H, Pócsi I, Kniemeyer O, Emri T. 2018.
567 Additional oxidative stress reroutes the global response of *Aspergillus fumigatus* to iron
568 depletion. BMC Genomics 19:357.

569 22. Basenko EY, Shanmugasundram A, Böhme U, Starns D, Wilkinson PA, Davison HR,
570 Crouch K, Maslen G, Harb OS, Amos B, McDowell MA, Kissinger JC, Roos DS, Jones A.
571 2024. What is new in FungiDB: a web-based bioinformatics platform for omics-scale
572 data analysis for fungal and oomycete species. Genetics 227:iyae035.

573 23. Scotto–Lavino E, Du G, Frohman MA. 2006. 3' End cDNA amplification using classic
574 RACE. Nat Protoc 1:2742–2745.

575 24. Kang Y-J, Yang D-C, Kong L, Hou M, Meng Y-Q, Wei L, Gao G. 2017. CPC2: a fast and
576 accurate coding potential calculator based on sequence intrinsic features. Nucleic
577 Acids Res 45:W12–W16.

578 25. Wang L, Park HJ, Dasari S, Wang S, Kocher J-P, Li W. 2013. CPAT: Coding-Potential
579 Assessment Tool using an alignment-free logistic regression model. Nucleic Acids Res
580 41:e74.

581 26. Sugareva V, Härtl A, Brock M, Hübner K, Rohde M, Heinekamp T, Brakhage AA. 2006.
582 Characterisation of the laccase-encoding gene abr2 of the dihydroxynaphthalene-like
583 melanin gene cluster of *Aspergillus fumigatus*. Arch Microbiol 186:345–355.

584 27. Long N, Xu X, Qian H, Zhang S, Lu L. 2016. A Putative Mitochondrial Iron Transporter
585 MrsA in Aspergillus fumigatus Plays Important Roles in Azole-, Oxidative Stress
586 Responses and Virulence. Front Microbiol 7.

587 28. Sasse C, Bastakis E, Bakti F, Höfer AM, Zangl I, Schüller C, Köhler AM, Gerke J,
588 Krappmann S, Finkernagel F, Harting R, Strauss J, Heimel K, Braus GH. 2023. Induction
589 of *Aspergillus fumigatus* zinc cluster transcription factor OdrA/Mdu2 provides
590 combined cellular responses for oxidative stress protection and multiple antifungal
591 drug resistance. mBio 14:e0262823.

592 29. Carrasco-Navarro U, Aguirre J. 2021. H2O2 Induces Major Phosphorylation Changes in
593 Critical Regulators of Signal Transduction, Gene Expression, Metabolism and
594 Developmental Networks in *Aspergillus nidulans*. Journal of Fungi 7:624.

595 30. Linder T. 2018. Evaluation of the chitin-binding dye Congo red as a selection agent for
596 the isolation, classification, and enumeration of ascomycete yeasts. Archives of
597 Microbiology 200:671.

598 31. Shlezinger N, Hohl TM. Mitochondrial Reactive Oxygen Species Enhance Alveolar
599 Macrophage Activity against *Aspergillus fumigatus* but Are Dispensable for Host
600 Protection. mSphere 6:e00260-21.

601 32. Hatinguais R, Pradhan A, Brown GD, Brown AJP, Warris A, Shekhova E. 2021.
602 Mitochondrial Reactive Oxygen Species Regulate Immune Responses of Macrophages
603 to *Aspergillus fumigatus*. Front Immunol 12.

604 33. Jhingran A, Mar KB, Kumasaka DK, Knoblaugh SE, Ngo LY, Segal BH, Iwakura Y, Lowell
605 CA, Hamerman JA, Lin X, Hohl TM. 2012. Tracing Conidial Fate and Measuring Host Cell
606 Antifungal Activity Using a Reporter of Microbial Viability in the Lung. Cell Rep 2:1762–
607 1773.

608 34. Zhai P, Shi L, Zhong G, Jiang J, Zhou J, Chen X, Dong G, Zhang L, Li R, Song J. 2021. The
609 OxrA Protein of *Aspergillus fumigatus* Is Required for the Oxidative Stress Response and
610 Fungal Pathogenesis. Applied and Environmental Microbiology 87:e01120-21.

611 35. Earle K, Valero C, Conn DP, Vere G, Cook PC, Bromley MJ, Bowyer P, Gago S.
612 Pathogenicity and virulence of *Aspergillus fumigatus*. Virulence 14:2172264.

613 36. Durieux M-F, Melloul É, Jemel S, Roisin L, Dardé M-L, Guillot J, Dannaoui É, Botterel F.
614 *Galleria mellonella* as a screening tool to study virulence factors of *Aspergillus*
615 *fumigatus*. Virulence 12:818–834.

616 37. Scotto–Lavino E, Du G, Frohman MA. 2006. 5' end cDNA amplification using classic
617 RACE. Nat Protoc 1:2555–2562.

618 38. Dhingra S, Andes D, Calvo AM. 2012. VeA regulates conidiation, gliotoxin production,
619 and protease activity in the opportunistic human pathogen *Aspergillus fumigatus*.
620 Eukaryot Cell 11:1531–1543.

621 39. Diederichs S. 2014. The four dimensions of noncoding RNA conservation. Trends in
622 Genetics 30:121–123.

623 40. Graf J, Kretz M. 2020. From structure to function: Route to understanding lncRNA
624 mechanism. BioEssays 42:2000027.

625 41. Novikova IV, Hennelly SP, Sanbonmatsu KY. 2012. Sizing up long non-coding RNAs.
626 Bioarchitecture 2:189–199.

627 42. Tassinari M, Richter SN, Gandellini P. 2021. Biological relevance and therapeutic
628 potential of G-quadruplex structures in the human noncoding transcriptome. Nucleic
629 Acids Res 49:3617–3633.

630 43. Wan Y, Kertesz M, Spitale RC, Segal E, Chang H. 2011. Understanding the transcriptome
631 through RNA structure. Nat Rev Genet 12:10.1038/nrg3049.

632 44. Statello L, Guo C-J, Chen L-L, Huarte M. 2021. Gene regulation by long non-coding
633 RNAs and its biological functions. Nat Rev Mol Cell Biol 22:96–118.

634 45. Baba SK, Baba SK, Mir R, Elfaki I, Algehainy N, Ullah MF, Barnawi J, Altemani FH, Alanazi
635 M, Mustafa SK, Masoodi T, Akil ASA, Bhat AA, Macha MA. 2023. Long non-coding RNAs
636 modulate tumor microenvironment to promote metastasis: novel avenue for
637 therapeutic intervention. Front Cell Dev Biol 11.

638 46. Liu L, Zhang Y, Lu J. 2020. The roles of long noncoding RNAs in breast cancer
639 metastasis. Cell Death Dis 11:749.

640 47. Gao N, Li Y, Li J, Gao Z, Yang Z, Li Y, Liu H, Fan T. 2020. Long Non-Coding RNAs: The
641 Regulatory Mechanisms, Research Strategies, and Future Directions in Cancers. Front
642 Oncol 10.

643 48. Yang J, Qi M, Fei X, Wang X, Wang K. 2021. Long non-coding RNA XIST: a novel oncogene
644 in multiple cancers. Molecular Medicine 27:159.

645 49. Muller HJ. 1932. Further studies on the nature and causes of gene mutations.

646 50. Pfaller MA, Messer SA, Boyken L, Rice C, Tendolkar S, Hollis RJ, Diekema DJ. 2008. In
647 Vitro Survey of Triazole Cross-Resistance among More than 700 Clinical Isolates of
648 *Aspergillus* Species. Journal of Clinical Microbiology 46:2568–2572.

649 51. Ballard E, Melchers WJG, Zoll J, Brown AJP, Verweij PE, Warris A. 2018. In-host
650 microevolution of *Aspergillus fumigatus*: A phenotypic and genotypic analysis. Fungal
651 Genet Biol 113:1–13.

652 52. Pelaez T, Gijón P, Bunsow E, Bouza E, Sánchez-Yebra W, Valerio M, Gama B, Cuenca-
653 Estrella M, Mellado E. 2012. Resistance to Voriconazole Due to a G448S Substitution in
654 *Aspergillus fumigatus* in a Patient with Cerebral Aspergillosis. J Clin Microbiol 50:2531–
655 2534.

656 53. Mellado E, Garcia-Effron G, Alcazar-Fuoli L, Cuenca-Estrella M, Rodriguez-Tudela JL.
657 2004. Substitutions at Methionine 220 in the 14α-Sterol Demethylase (Cyp51A) of
658 *Aspergillus fumigatus* Are Responsible for Resistance In Vitro to Azole Antifungal Drugs.
659 Antimicrob Agents Chemother 48:2747–2750.

660 54. Rajendran R, Mowat E, McCulloch E, Lappin DF, Jones B, Lang S, Majithiya JB, Warn P,
661 Williams C, Ramage G. 2011. Azole Resistance of *Aspergillus fumigatus* Biofilms Is
662 Partly Associated with Efflux Pump Activity. Antimicrobial Agents and Chemotherapy
663 55:2092–2097.

664 55. Campoli P, Al Abdallah Q, Robitaille R, Solis NV, Fielhaber JA, Kristof AS, Laverdiere M,
665 Filler SG, Sheppard DC. 2011. Concentration of Antifungal Agents within Host Cell
666 Membranes: a New Paradigm Governing the Efficacy of Prophylaxis ▿. Antimicrob
667 Agents Chemother 55:5732–5739.

668 56. Perfect JR, Savani DV, Durack DT. 1993. Uptake of itraconazole by alveolar
669 macrophages. Antimicrob Agents Chemother 37:903–904.

670 57. Xiao L, Madison V, Chau AS, Loebenberg D, Palermo RE, McNicholas PM. 2004. Three-
671 Dimensional Models of Wild-Type and Mutated Forms of Cytochrome P450 14α-Sterol
672 Demethylases from *Aspergillus fumigatus* and *Candida albicans* Provide Insights into
673 Posaconazole Binding. Antimicrob Agents Chemother 48:568–574.

674 58. Douglas CM, Foor F, Marrinan JA, Morin N, Nielsen JB, Dahl AM, Mazur P, Baginsky W, Li
675 W, el-Sherbeini M. 1994. The *Saccharomyces cerevisiae* FKS1 (ETG1) gene encodes an
676 integral membrane protein which is a subunit of 1,3-beta-D-glucan synthase. Proc Natl
677 Acad Sci U S A 91:12907–12911.

678 59. Kelly R, Register E, Hsu MJ, Kurtz M, Nielsen J. 1996. Isolation of a gene involved in 1,3-
679 beta-glucan synthesis in *Aspergillus nidulans* and purification of the corresponding
680 protein. Journal of Bacteriology 178:4381–4391.

681 60. Sijacic P, Wang W, Liu Z. 2011. Recessive Antimorphic Alleles Overcome Functionally
682 Redundant Loci to Reveal TSO1 Function in Arabidopsis Flowers and Meristems. PLoS
683 Genet 7:e1002352.

684 61. Steele C, Rapaka RR, Metz A, Pop SM, Williams DL, Gordon S, Kolls JK, Brown GD. 2005.
685 The Beta-Glucan Receptor Dectin-1 Recognizes Specific Morphologies of *Aspergillus*
686 *fumigatus*. PLoS Pathog 1:e42.

687 62. Batbayar S, Lee DH, Kim HW. 2012. Immunomodulation of Fungal β-Glucan in Host
688 Defense Signaling by Dectin-1. Biomol Ther (Seoul) 20:433–445.

689 63. Becker KL, Aimanianda V, Wang X, Gresnigt MS, Ammerdorffer A, Jacobs CW,
690 Gazendam RP, Joosten LAB, Netea MG, Latgé JP, van de Veerdonk FL. 2016. *Aspergillus*
691 Cell Wall Chitin Induces Anti- and Proinflammatory Cytokines in Human PBMCs via the
692 Fc-γ Receptor/Syk/PI3K Pathway. mBio 7:e01823-15.

693 64. Wagener J, Malireddi RKS, Lenardon MD, Köberle M, Vautier S, MacCallum DM,
694 Biedermann T, Schaller M, Netea MG, Kanneganti T-D, Brown GD, Brown AJP, Gow NAR.
695 2014. Fungal Chitin Dampens Inflammation through IL-10 Induction Mediated by NOD2
696 and TLR9 Activation. PLOS Pathogens 10:e1004050.

697 65. Donaldson ME, Saville BJ. 2013. *Ustilago maydis* natural antisense transcript
698 expression alters mRNA stability and pathogenesis. Mol Microbiol 89:29–51.

699 66. Chacko N, Zhao Y, Yang E, Wang L, Cai JJ, Lin X. 2015. The lncRNA RZE1 Controls
700 Cryptococcal Morphological Transition. PLoS Genet 11:e1005692.

701 67. Wang Y, Shao Y, Zhu Y, Wang K, Ma B, Zhou Q, Chen A, Chen H. 2019. XRN1-associated
702 long non-coding RNAs may contribute to fungal virulence and sexual development in
703 entomopathogenic fungus *Cordyceps militaris*. Pest Manag Sci 75:3302–3311.

704 68. Paris S, Wysong D, Debeaupuis J-P, Shibuya K, Philippe B, Diamond RD, Latgé J-P. 2003.
705 Catalases of *Aspergillus fumigatus*. Infect Immun 71:3551–3562.

706 69. Lambou K, Lamarre C, Beau R, Dufour N, Latge J-P. 2010. Functional analysis of the
707 superoxide dismutase family in *Aspergillus fumigatus*. Molecular Microbiology 75:910–
708 923.

709 70. Zhai P, Shi L, Zhong G, Jiang J, Zhou J, Chen X, Dong G, Zhang L, Li R, Song J. The OxrA
710 Protein of *Aspergillus fumigatus* Is Required for the Oxidative Stress Response and
711 Fungal Pathogenesis. Appl Environ Microbiol 87:e01120-21.

712 71. Zepeda B, Verdonk JC. 2022. RNA Extraction from Plant Tissue with Homemade Acid
713 Guanidinium Thiocyanate Phenol Chloroform (AGPC). Current Protocols 2:e351.

714 72. Barratt RW, Johnson GB, Ogata WN. 1965. Wild-Type and Mutant Stocks of *Aspergillus*
715 *nidulans*. Genetics 52:233–246.

716 73. Bertuzzi M, van Rhijn N, Krappmann S, Bowyer P, Bromley MJ, Bignell EM. 2020. On the
717 lineage of *Aspergillus fumigatus* isolates in common laboratory use. Med Mycol 59:7–
718 13.

719 74. Punt PJ, Dingemanse MA, Kuyvenhoven A, Soede RDM, Pouwels PH, van den Hondel
720 CAMJJ. 1990. Functional elements in the promoter region of the *Aspergillus nidulans*
721 *gpdA* gene encoding glyceraldehyde-3-phosphate dehydrogenase. Gene 93:101–109.

722 75. Szewczyk E, Nayak T, Oakley CE, Edgerton H, Xiong Y, Taheri-Talesh N, Osmani SA,
723 Oakley BR. 2006. Fusion PCR and gene targeting in *Aspergillus nidulans*. Nat Protoc
724 1:3111–3120.

76. Hill T, Kafer E. 2001. Improved protocols for *Aspergillus* minimal medium: trace element and minimal medium salt stock solutions. Fungal Genetics Reports 48:20–21.

77. Sambrook J. 2001. Molecular cloning : a laboratory manual. Third edition. Cold Spring Harbor, N.Y. : Cold Spring Harbor Laboratory Press, [2001] ©2001. https://search.library.wisc.edu/catalog/999897924602121.

732 **Figure legends:**

733 Figure 1. *afu-254* is an lncRNA that regulates fungal oxidative stress response. (A) 5' and 3'
734 rapid amplification of cDNA ends confirmed the boundary of *afu-254* in the genome as
735 indicated. (B) qPCR analysis showing the relative levels of *afu-254* in the presence of
736 oxidative stress compared to GMM. Student's t-test was used to compare the differences in
737 the mean. Fungal strains were inoculated in top agar. After solidification, a core was cut in
738 the center using a sterile pipette tip, and 100μl of either (C) 5mM H_2O_2 or (D) 2mM
739 menadione was added. The zone of inhibition was measured after 36 hours and
740 represented. One-Way ANOVA followed by Tukey's post-hoc test was used to compare
741 differences in the mean. ** $p<0.01$, *** $p<0.001$, ns – not significant

742

743 Figure 2. OE-254 constitutes an antimorph. (A) WT and OE-254 RNA were loaded in a
744 denaturing formaldehyde gel at the indicated concentration. The samples were heated at
745 65°C for 5 min before loading and were probed with DIG-labeled *afu-254* sequence. The
746 chemiluminscenc image was captured using Azure C300 imaging system. The OE-254
747 strain shows the presence of a higher molecular weight band (red arrow). (B) The samples
748 were heated at 98°C for 15 mins, leading to loss of the higher molecular weight band. (C
749 and D). RNA was loaded in denaturing agarose gel and was imaged before transfer to the
750 nylon membrane. rRNA bands are shown for quality and quantity of loaded RNA.

751

752 Figure 3. *afu-254* plays a role in fungal response to posaconazole and itraconazole on solid
753 medium and surface attached cultures. Fungal strains were spot inoculated (10^4 spores) in
754 (A) absence of drug or presence of (B and C) posaconazole or (D and E) Itraconazole. Both
755 Δ*afu-254* and OE-254 show increased susceptibility to long tailed azoles. (D and E)
756 Quantitative measurements of fungal growth after 48 hours are represented as a ratio of
757 fungal growth in the presence and absence of the indicated drug. (F) *afu-254* plays a role in
758 fungal surface attachment. Fungal strains were allowed to adhere to the abiotic surface for
759 12 hours. The surface attached cultures were then (F) left untreated (GMM), treated with
760 posaconazole for 8 hours (GMM + 0.2μg/ml posaconazole), washed and stained with
761 crystal violet. (F) Values represent the absorbance of untreated samples. The OE-254 strain
762 shows decreased surface attachment. (G) Values represent the ratio between absorbance
763 measured after azole treatment and fungal attachment before treatment at the 12-hour
764 time point. a.u. – arbitrary units. One-Way ANOVA followed by Tukey's post-hoc test was
765 used to compare differences in the mean. **** $p<0.0001$.

766

767 Figure 4. *afu-254* mediates fungal cell wall response to Congo red but not to Caspofungin.
768 Fungal strains were spot inoculated (10^4 spores) in a 24 well plate in the absence or
769 presence of indicated concentrations of (A) Congo red or (C). Caspofungin. Both Δ*afu-254*
770 and OE-254 strains are susceptible to Congo red (red arrows) but not to Caspofungin. (B)
771 Quantitative analysis of fungal growth is represented as a ratio between growth in the
772 presence of CR and the absence of CR. One-Way ANOVA followed by Tukey's post-hoc test
773 was used to compare differences in the mean. ** $p<0.01$, **** $p<0.0001$.

774

775 Figure 5: *afu-254* regulates fungal *ex vivo* killing and virulence in an invertebrate model of
776 infection. BMDMs were incubated with conidia from the indicated strain (5:1 conidia to cell)
777 that were biotinylated and stained with AF633 for 3 hrs. Cells were collected, and the
778 percentage of live BMDMs (A) with (uptake) or (B) without (empty) conidia was determined
779 by gating on AF633+ vs AF633- BMDMs using flow cytometry. The Δ*afu-254* strain showed
780 less uptake by BMDMs. The points represent combined data from 2 experiments. (C)
781 BMDMs were incubated with conidia from the indicated strains (5:1 conidia to cell) for 5
782 hrs. Cells were lysed, and CFUs were determined by serial dilution and plating. Results
783 depict the percentage of killed conidia from three independent experiments compared to
784 the starting inoculum. The OE-254 strain shows statistically increased killing by BMDMs,
785 whereas the Δ*afu-254* strain trends towards increased killing, albeit not statistically
786 significant. The Kruskal-Wallis test with Dunn's multiple comparisons was performed for
787 statistical analyses. All error bars represent standard error. * $p<0.05$, **** $p<0.0001$. (D)
788 *afu-254* plays a role in virulence. *Galleria mellonella* larvae were infected with the 5×10^4
789 spores of the indicated strains of *A. fumigatus* and monitored. The larvae exhibiting a lack
790 of movement upon physical stimuli were marked as dead (n=20 for all infected larvae, 10
791 for controls). Log-rank test was used to determine survival distribution and survival was
792 significantly different for the Δ*afu-254* strain and the OE-254 strain compared to WT
793 ($p<0.001$ and $p<0.0001$, respectively).

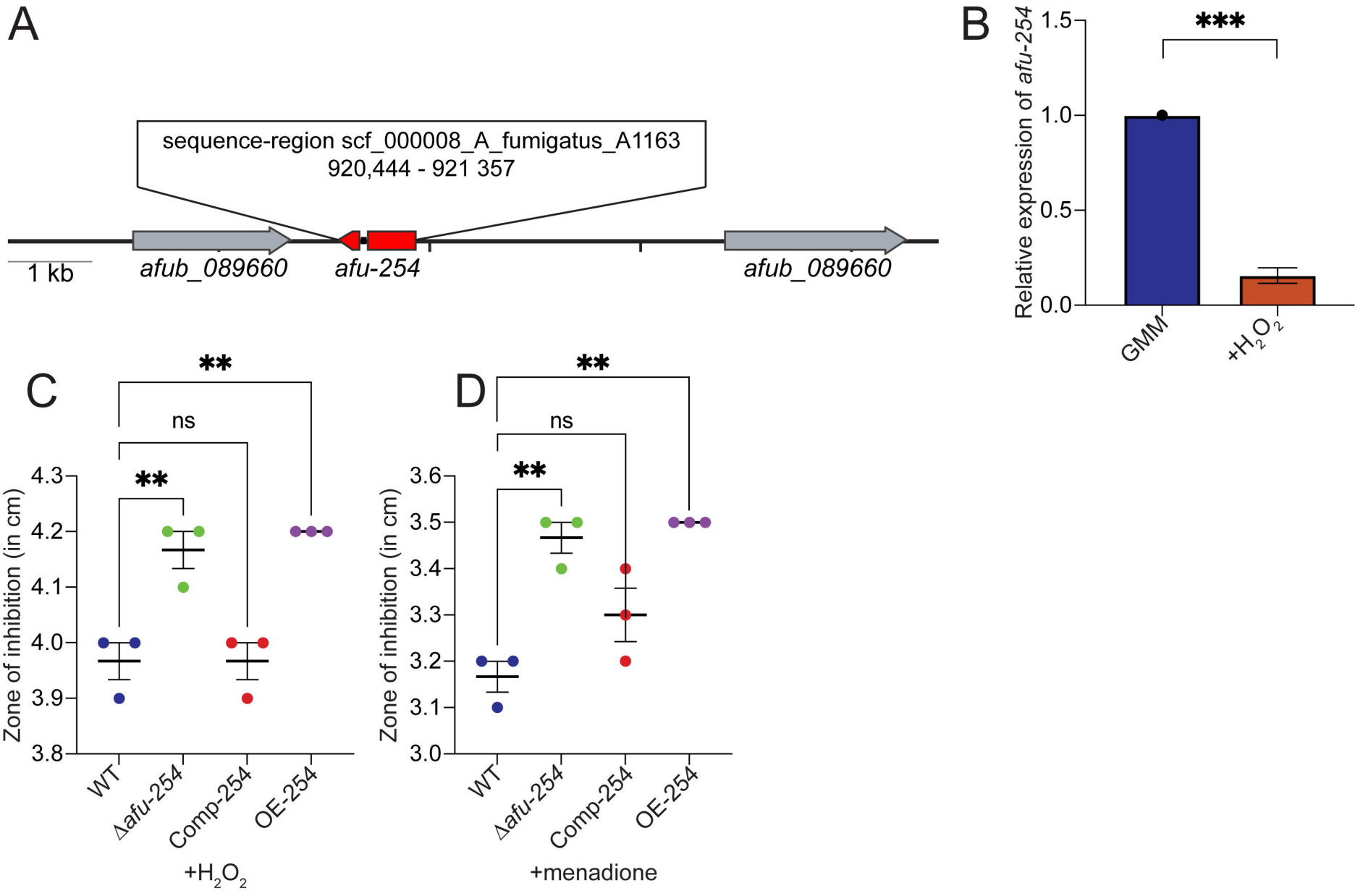
A
sequence-region scf_000008_A_fumigatus_A1163
920,444 - 921 357
1 kb
afub_089660
afu-254
afub_089660
B
Relative expression of afu-254
1.5
1.0
0.5
0.0
***
GMM
+H2O2
C
**
ns
**
Zone of inhibition (in cm)
4.3
4.2
4.1
4.0
3.9
3.8
WT
Δafu-254
Comp-254
OE-254
+H2O2
D
**
ns
**
Zone of inhibition (in cm)
3.6
3.5
3.4
3.3
3.2
3.1
3.0
WT
Δafu-254
Comp-254
OE-254
+menadione

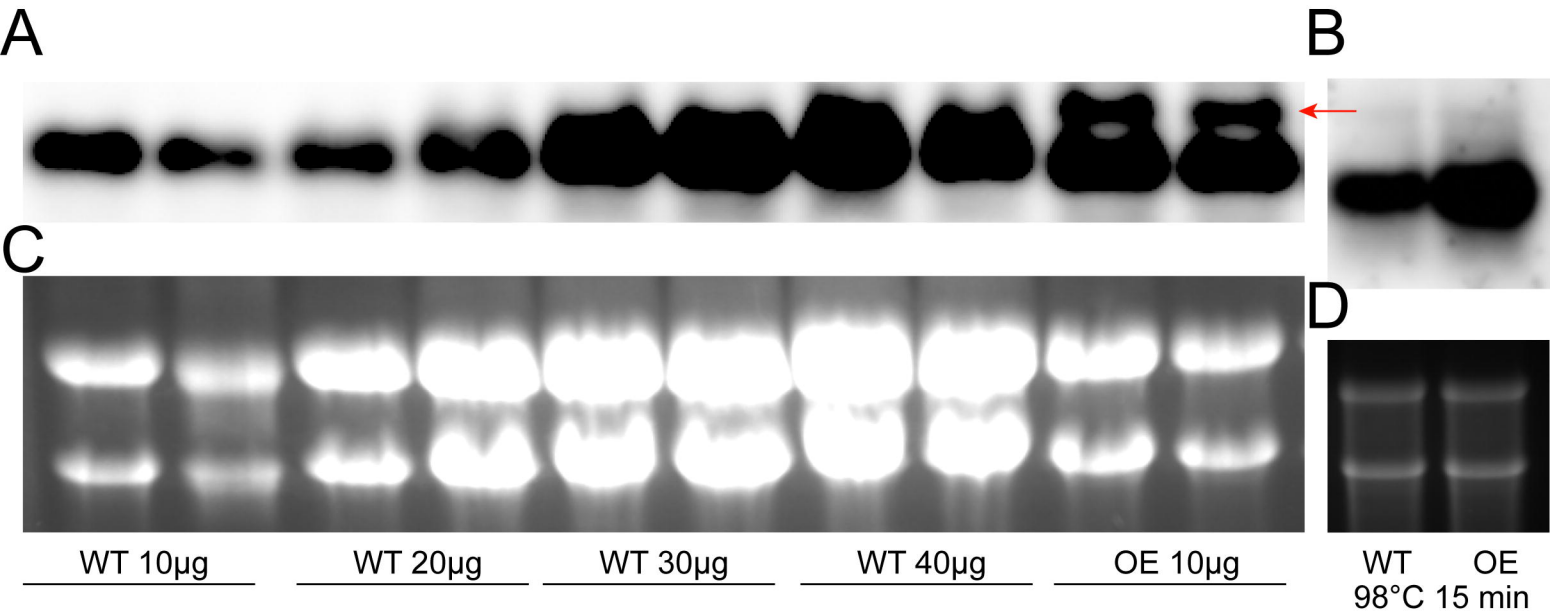
A
B
C
D
WT 10μg
WT 20μg
WT 30μg
WT 40μg
OE 10μg
WT
OE
98°C 15 min

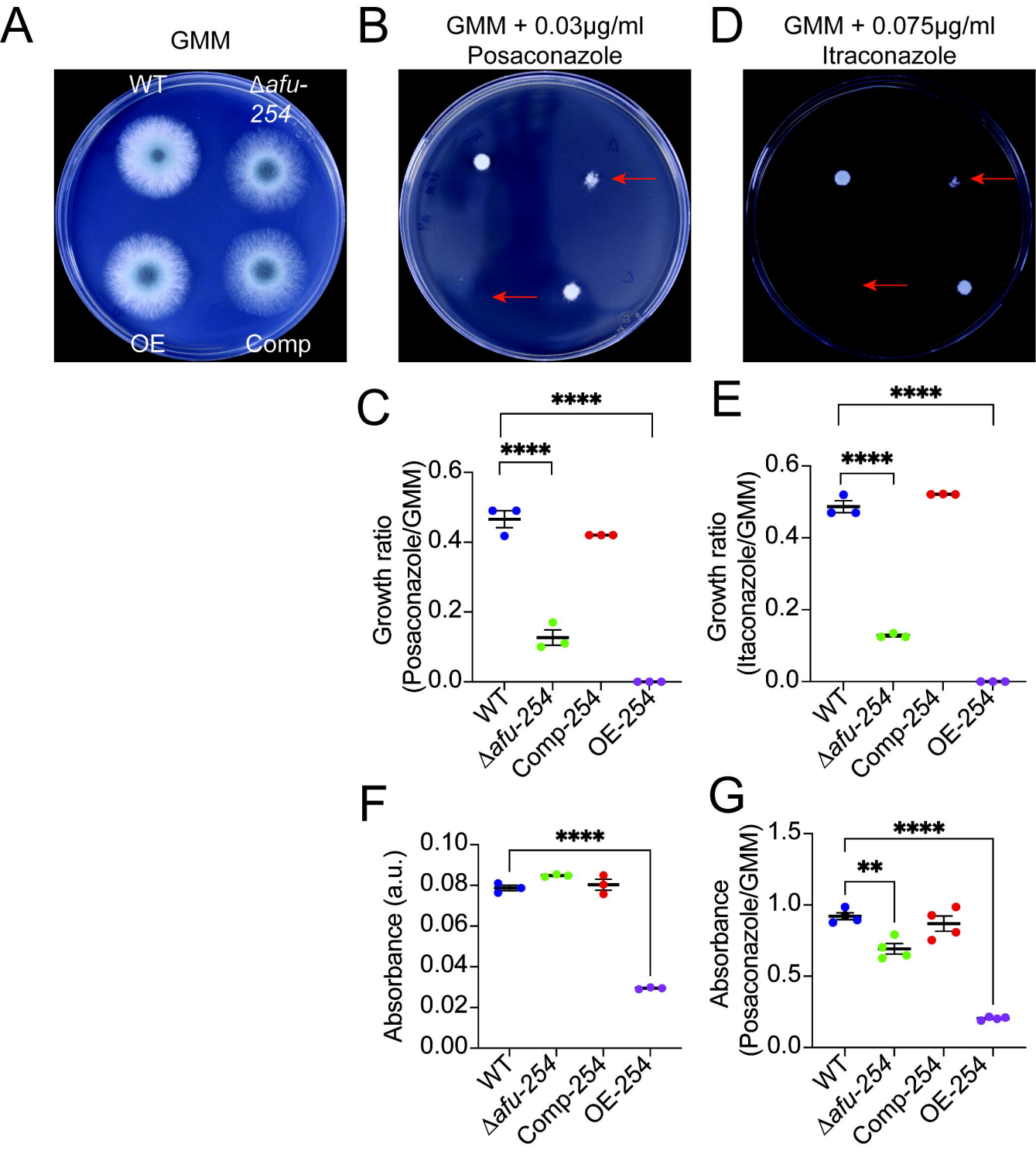
A
GMM
WT
Δafu-254
OE
Comp
B
GMM + 0.03μg/ml Posaconazole
D
GMM + 0.075μg/ml Itraconazole
C
****
****
Growth ratio (Posaconazole/GMM)
0.6
0.4
0.2
0.0
WT
Δafu-254
Comp-254
OE-254
E
****
****
Growth ratio (Itaconazole/GMM)
0.6
0.4
0.2
0.0
WT
Δafu-254
Comp-254
OE-254
F
****
Absorbance (a.u.)
0.10
0.08
0.06
0.04
0.02
0.00
WT
Δafu-254
Comp-254
OE-254
G
****
**
Absorbance (Posaconazole/GMM)
1.5
1.0
0.5
0.0
WT
Δafu-254
Comp-254
OE-254

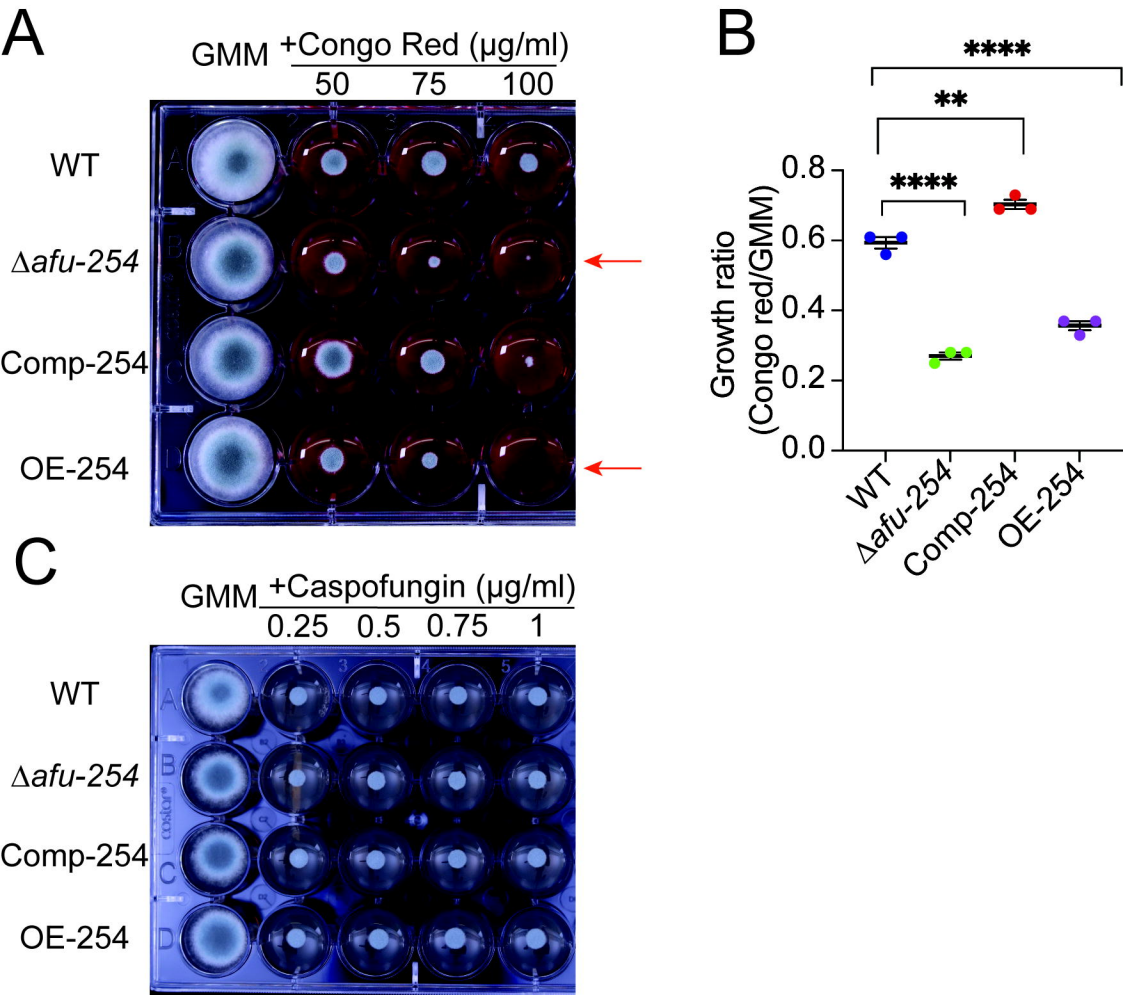
A
GMM
+Congo Red (μg/ml)
50
75
100
WT
Δafu-254
Comp-254
OE-254
B
****
**
****
Growth ratio
(Congo red/GMM)
0.8
0.6
0.4
0.2
0.0
WT
Δafu-254
Comp-254
OE-254
C
GMM
+Caspofungin (μg/ml)
0.25
0.5
0.75
1
WT
Δafu-254
Comp-254
OE-254

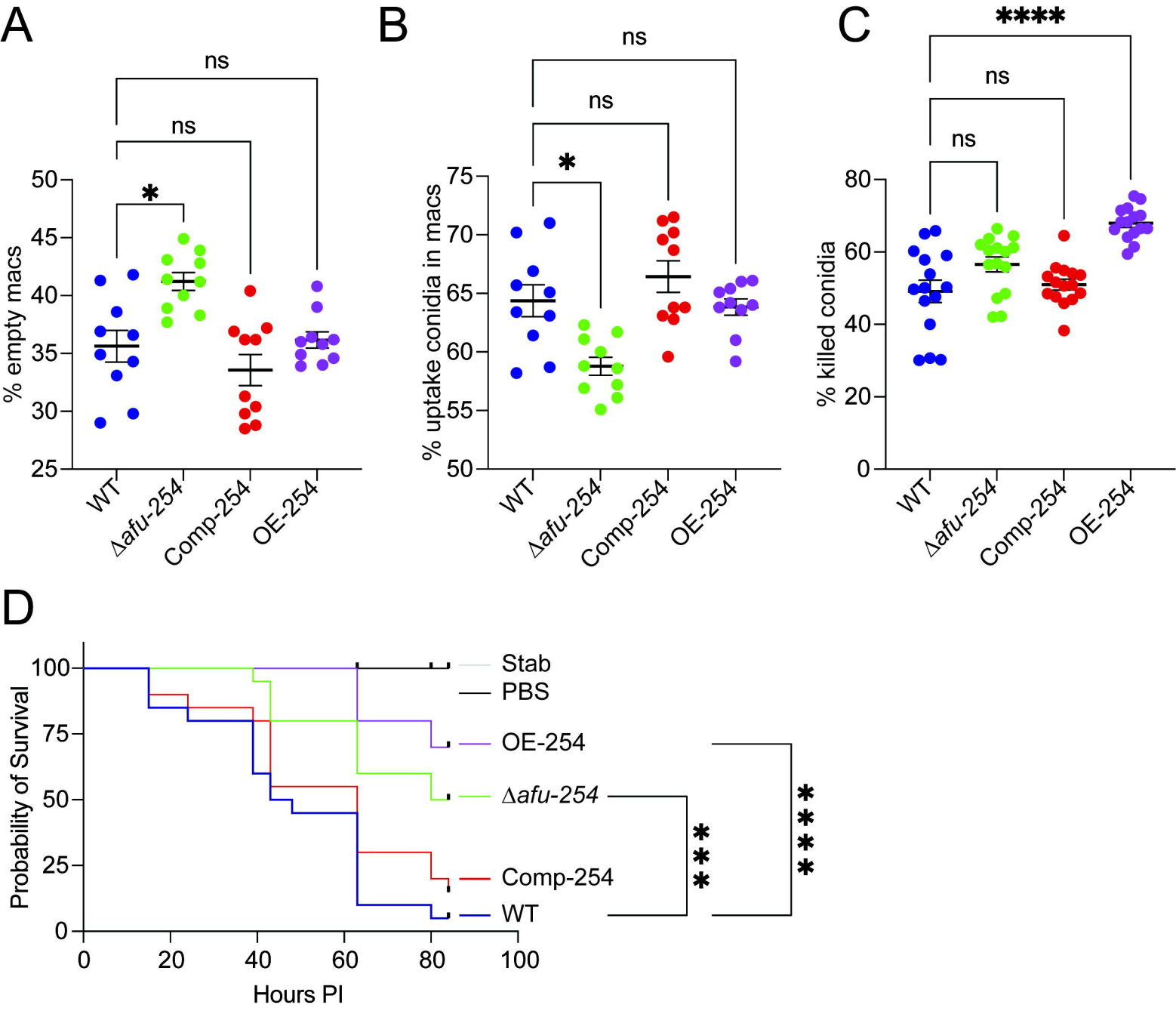
A
ns
ns
*
% empty macs
50
45
40
35
30
25
WT
Δafu-254
Comp-254
OE-254
B
ns
ns
*
% uptake conidia in macs
75
70
65
60
55
50
WT
Δafu-254
Comp-254
OE-254
C
****
ns
ns
% killed conidia
80
60
40
20
0
WT
Δafu-254
Comp-254
OE-254
D
Probability of Survival
100
75
50
25
0
0
20
40
60
80
100
Hours PI
Stab
PBS
OE-254
Δafu-254
Comp-254
WT
****
****